

Simulation of a Simple Wolter Telescope of Type I by Geant4 for Some Widely Used Materials

Mehdi Abbasian Motlagh¹ · Gohar Rastegarzadeh²

¹ Department of Physics, University of Semnan, Semnan, Iran;
email: abbasianmotlagh@semnan.ac.ir

² Department of Physics, University of Semnan, Semnan, Iran;
email: grastegar@semnan.ac.ir

Abstract. At the present work, the reflection of X-rays from surfaces composed of silicon, gold, iridium, and nickel is simulated in the range of $E \leq 5$ keV energy for the two cases, which includes raw mirror surfaces and a typical Wolter-I optics-based X-ray telescope. We used Geant4 and a proper optical extension to use Geant4 as a general-purpose X-ray tracing package. The reflectivity of the materials and the efficiency of the telescope for the materials have been obtained as a function of energy. Except for silicon, the efficiencies are close to each other for the materials. Of course, we generally see a larger value for nickel. Due to the importance of Wolter-I optics in the simulation of X-ray telescopes and enhancement of the sensitivity of X-ray telescopes by increasing the reflectivity, the results of the present study have particular use in the manufacturing process of an X-ray telescope.

Keywords: X-ray Telescope, Geant4, Simulation, Wolter Optics, X-ray tracing

1 Introduction

Geant4 is a platform for the simulation of the passage of particles through matter. The package is developed by an international collaboration under the supervision of CERN [1]. The importance of simulations in the development, fabrication, testing, and performance of X-ray optics is well known. However, conventional telescope designs require reflection or refraction in a manner that does not work well for X-rays. A Wolter telescope is a telescope for X-rays that only uses grazing incidence optics – mirrors that reflect X-rays at very shallow angles (typically 10 arc-minutes to 2 degrees) [2]. Hans Wolter first described Wolter optics in 1952 [3], which quickly became the preferred configuration in X-ray imaging systems. Type I of Wolter optics consists of a pair of mirrors, one parabolic and the other hyperbolic so that the latter is placed next to the former (Fig. 1).

The incoming photons are first reflected by the parabolic mirror, which concentrates off-axis rays into an annulus. Then, the hyperbolic mirror brings the annulus to a point in the focal plane. These mirrors are relatively thin cylindrical shells with the inner surface having the shape of the paraboloid or hyperboloid. To increase the effective collecting area, several pairs of parabolic and hyperbolic mirrors can be nested (Fig. 2) [4]. This type of optics is the most common optics used in X-ray telescopes. For example, Fig. 3 shows what the mirror assembly for the XMM-Newton X-ray observatory looks like.

In 1972, the optical properties of Wolter optics were evaluated numerically for the first time. Then, several other authors, including Saha and Zhang, studied X-ray imaging systems. Apart from aberration-based properties and focalization capabilities that can be

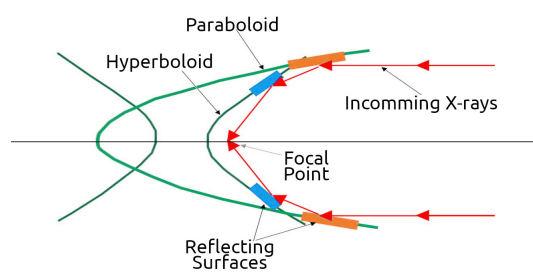


Figure 1: Type I of Wolter optics consists of a pair of mirrors, one parabolic and the other hyperbolic.

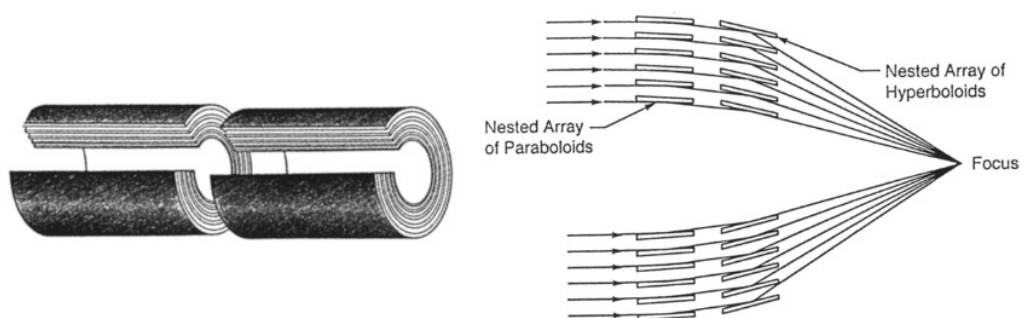


Figure 2: A Wolter-I mirror configuration showing nested paraboloids and hyperboloids.

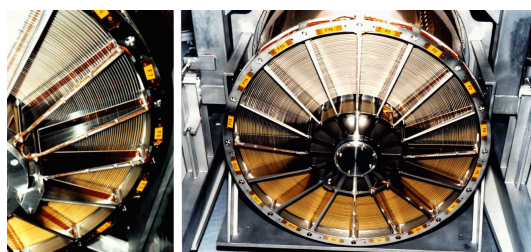


Figure 3: Photo of the XMM-Newton mirrors.

Table 1: The reflective surface material of mirrors in some X-ray telescopes.

Telescope	Einstein	Chandra	XMM	ATHENA
Material	Ni	Ir	Au	Si (as base material)

tested with standard optics tools, X-ray tracking tools need to be used to determine parameters, including Effective Area and Point Spread Function (PSF). These parameters are essential in assessing the performance of a system. In such tools, changes of reflectivity as a result of incidence angle modifications and scatterings that occur due to the type of surface finish are taken into account [5]. Depending on the design of Wolter-I optics-based X-ray telescopes, the beam focusing part is created by stacking the Wolter-I units. Therefore, studying these units is the first step in building this part of the telescope.

Over the past few decades, various space projects have included X-ray telescopes. Some of these projects have been designed specifically for X-ray exploration. Since X-rays get absorbed in the atmosphere, X-ray telescopes should be installed on balloons or satellites to reach the top of the Earth's atmosphere. The Sensitivity of a telescope is the lowest flux that can be detected and recorded by the telescope. It is, in fact, the lowest brightness that a telescope can detect. Telescopes with high sensitivity can detect feeble as well as very bright sources. For example, in the 0.52 keV band, the sensitivity for Chandra Deep Wide-Field Survey is about $1.5 \times 10^{-16} \text{ erg cm}^{-2} \text{ s}^{-1}$ [6], and the sensitivity of ATHENA X-ray telescope, which is expected to launch in 2031, is predicted to be $2.5 \times 10^{-17} \text{ erg cm}^{-2} \text{ s}^{-1}$ [7]. Since the sensitivity of a telescope depends entirely on its ability to collect light, studying the optical response of various telescope components is one of the most critical parts of any telescope design, including X-ray telescopes, to determine and increase its sensitivity. The sensitivity of an X-ray telescope decreases as the background flux increases and increases as the effective area of the telescope increases. Also, the effective area of the telescope increases in proportion to the square of reflectivity of the mirrors [8]. In addition, the type of material that forms the reflecting surface of mirrors affects reflectivity and thus the sensitivity of X-ray telescopes. Table 1 shows the reflective surface material of some X-ray telescopes. In Athena, silicon acts as a mirror substrate and the reflective surface is suitably coated by a high-Z element, e.g. gold or iridium.

The propagation of radiation is generally presented according to an optical formalism in which a refractive index describes the properties of a medium. Knowing the refractive index is sufficient to predict what will happen at an interface, that is to establish the Snell–Descartes' laws and to calculate the Fresnel coefficients for reflection and transmission [9]. The coefficients R and T for a photon with energy E, grazing incidence angle θ_i and refraction angle θ_t , are

$$R_{(\theta_i, E)} = \left| \frac{\sin \theta_i - n(E) \sin \theta_t}{\sin \theta_i + n(E) \sin \theta_t} \right|^2 \quad T_{(\theta_i, E)} = \left| \frac{2 \sin \theta_i}{\sin \theta_i + n(E) \sin \theta_t} \right|^2 \quad (1)$$

with each θ as the angle measured from the surface of the medium and n as the refractive index of the medium. The reflection coefficient (R) given in Eq. 1 is valid in the case of an ideal and smooth surface. For a real surface, some fraction of the reflected photons will be scattered away from the specular direction. Under assumptions that are generally true for X-ray optics, it is customary to characterize a surface by its micro-roughness σ as the RMS

value of the surface height deviations, and decrease the reflectivity (R) by a factor

$$R_r = \exp\left(-\left(\frac{4\pi\sigma \sin \theta_i}{\lambda}\right)^2\right) R \quad (2)$$

where λ is the wavelength of X-ray [5].

In this paper, after a brief introduction about our code, we report the results of the simulations, followed by a conclusion.

2 Simulations and Results

Geant4 includes many physical processes but it lacks a description of the reflection of X-ray photons at a grazing incident angle. Buis and Vacanti [5] developed an extension called XRTG4 for Geant4 that allows it to be used as a general-purpose X-ray tracing package. In this extension, the physical process is realized through the implementation of three classes:

- **G4XrayRefractionIndex:** It manages the refraction index data for particular materials.
- **G4XraySurfaceProperty:** A derived object of G4SurfaceProperty allowing the definition of X-ray reflecting surfaces and is used to describe the microscopic surface details.
- **G4XrayGrazingAngleScattering:** This class models a new Geant4 boundary process and implements the grazing angle scattering of X-rays on the surface during which the reflectivity changes with the surface roughness, incident angle, and energy [10].

The main components of our X-ray tracing simulation code are:

- **Primary particles:** properties of X-rays, including energy, initial direction and position.
- **Physics processes:** describing how X-rays interact with materials by XRTG4 extension.
- **Volumes:** which are described by their shapes and their physical characteristics.

2.1 Simulation of the reflectivity of raw mirror surfaces used in X-ray telescopes

As mentioned in the previous section, the sensitivity of X-ray telescopes increases in proportion to the square of reflectivity. To study the dependence of reflectivity on the energy of incident X-rays as well as the material of mirrors, using the X-ray tracing simulation code in Geant4, the reflectivity of these surfaces was calculated by designing a simple structure consisting of an X-ray counter and a plate of the materials introduced in Table 1 with $\sigma = 1 \text{ nm}$. The code was executed in 491 different energies (0.1 - 5.0 keV). In each run, the ratio N/N_0 was obtained as the plates' reflectivity by shooting $N_0 = 100000$ X-rays with a grazing incidence angle of 1 degree and counting the number of X-rays which have reached the counter (N). The results were compared with the data made available by the Center for X-Ray Optics [11]. By exploring the contents of the plots (Figure 4), we found out that gold and iridium have a higher reflectivity than silicon at energies higher than 2.5 keV, where the difference between the curves of gold and iridium is quite small.

Figure 5 shows a comparison between the reflectivity of silicon, gold, iridium, and nickel obtained from the simulations. Except for nickel, at energies less than 1.5 keV the reflectivity is more than 0.9. The highest reflectivity in the range of 1.5 to 3 keV is for nickel. At higher energies, a decrease in reflectivity is observed for all materials.

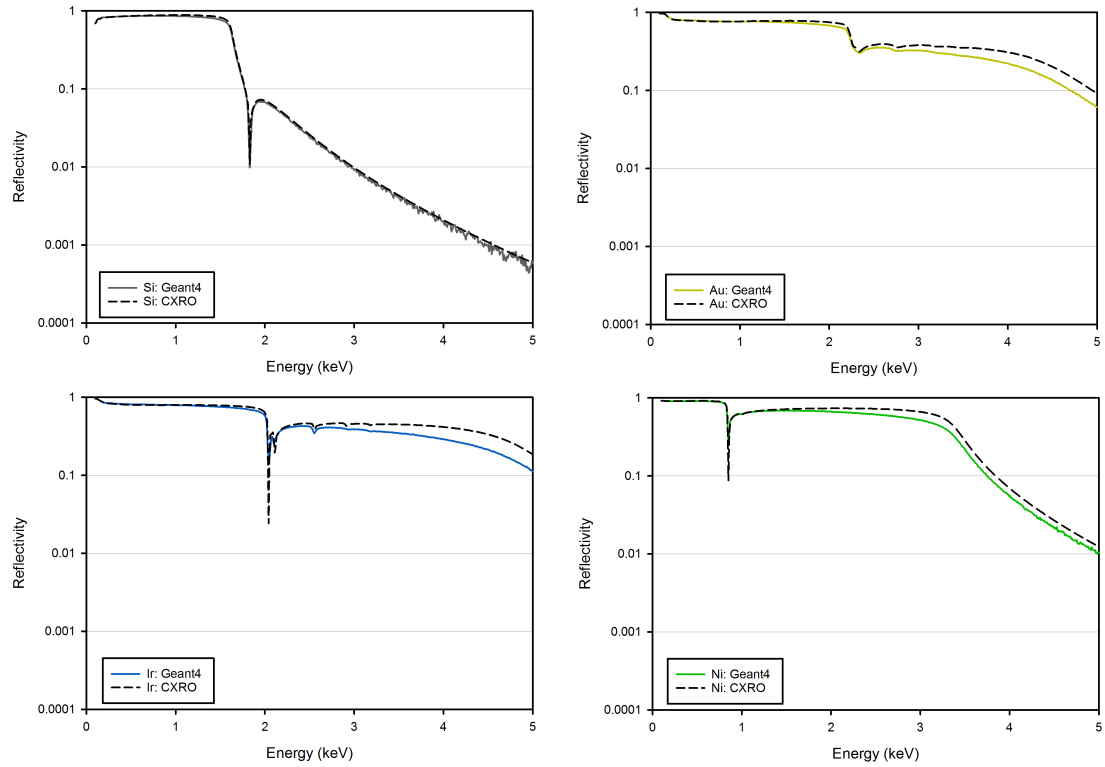


Figure 4: The reflectivity of silicon, gold, iridium and nickel determined from the simulation and obtained from the Center for X-Ray Optics.

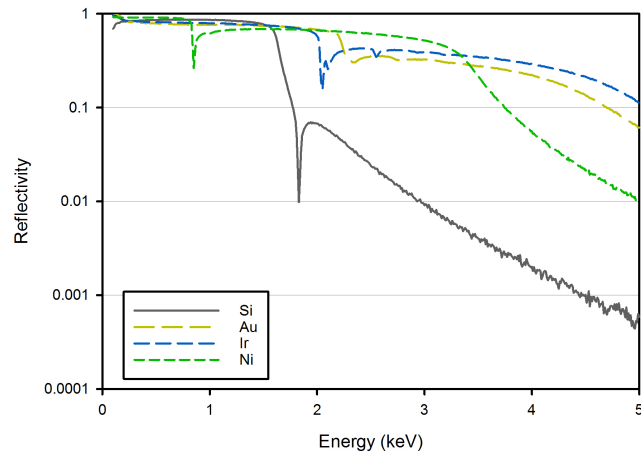


Figure 5: Comparison of the reflectivity of silicon, gold, iridium and nickel raw surfaces obtained from the plates simulation.

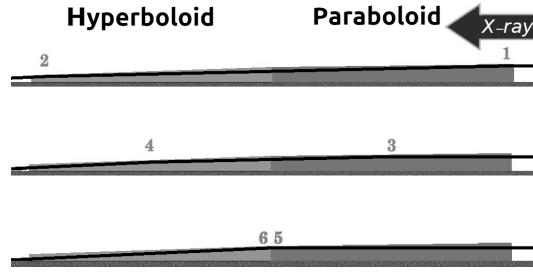


Figure 6: Dependence of positions of hits (the numbers 1-6) on distances of primary X-rays from the axis of the telescope. Top to bottom: decreasing the distances.

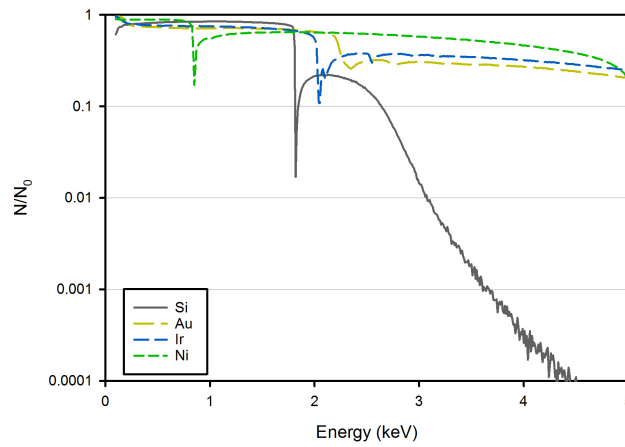


Figure 7: Comparison of the ratio N/N_0 for the silicon, gold, iridium, and nickel coatings on silicon substrate obtained by the Wolter-I optics-based X-ray telescope simulation.

2.2 Simulation of a Wolter-I Optics-Based X-ray Telescope

By running the code for a structure similar to which is shown in Figure 1, the efficiency of a simple Wolter telescope of type I was studied as a function of energy as well as the material of mirrors and also different distances of primary X-rays from the axis of the telescope and parallel to it which cause the different positions of hits (Figure 6).

Similar to the previous simulations, the code was executed in 491 different energies (0.1 - 5.0 keV) and in each run $N_0 = 100000$ X-rays were shot at three different distances from the axis of the telescope and parallel to it. By counting the number of X-rays which have reached the counter (N), the ratio N/N_0 was obtained for silicon substrates with silicon, gold, iridium and nickel coatings with $\sigma = 1 \text{ nm}$. By exploring the contents of plots, no difference in the ratio N/N_0 was observed for different distances from the axis. However, given that there is limited space between Wolter-I units in the ray-bending part of the telescope, this result may not apply to it for all cases. Figure 7 shows the ratio N/N_0 for the silicon, gold, iridium, and nickel coatings obtained from the simulations. Except for silicon, the ratio lines are close to each other for coatings made of the elements. Of course,

we generally see a larger value for nickel.

3 Conclusion

Reflectivity as an effective component in the sensitivity and, consequently, X-ray telescopes' efficiency was investigated for some widely used materials in their mirrors. The result is in agreement with the data made available by the Center for X-Ray Optics. In particular, the need to use high-reflectivity materials as surface coatings for silicon in Athena and, in general, for Wolter-I optics-based telescopes was determined. It is necessary to implement the beam focusing part of the telescope by assembling the Wolter-I units in simulations to assess parameters such as effective area. The next step of the research is to implement the beam focusing part of the telescope in the code and determine the parameters that affect the telescope performance.

References

- [1] Agostinelli, S., & et al. 2003, Nucl. Instrum. Methods Phys. Res., Sect. A, 506, 250.
- [2] Singh, K. P. 2005, Resonance, 10, 8.
- [3] Wolter, H. 1952, Annalen der Physik, 445, 94.
- [4] Ramsey, B. D., Austin, R. A., & Decher, R. 1994, Space Sci. Rev., 69, 139.
- [5] Buis, E., & Vacanti, G. 2009, Nucl. Instrum. Methods Phys. Res., Sect. A, 599, 260.
- [6] Masini, A., & et al. 2020, ApJS, 251, 2.
- [7] Matt, G. 2019, Astron. Nachr. 340, 35.
- [8] Malaguti, G., & et al. 2005, Proceedings of the SPIE, 5900, 159.
- [9] Daillant, J., & Gibaud, A. 2008, X-ray and neutron reflectivity: principles and applications, Springer.
- [10] Zhao, D., & et al. 2017, Exp. Astron., 43, 267.
- [11] https://henke.lbl.gov/optical_constants.